

*Letter to the Editor***Molecular gas in the Cartwheel Galaxy\***C. Horellou<sup>1</sup>, V. Charmandaris<sup>2</sup>, F. Combes<sup>2</sup>, P.N. Appleton<sup>3</sup>, F. Casoli<sup>2</sup>, and I.F. Mirabel<sup>4,5</sup><sup>1</sup> Onsala Space Observatory, Chalmers University of Technology, S-43992 Onsala, Sweden<sup>2</sup> Observatoire de Paris, DEMIRM, 61 Avenue de l'Observatoire, F-75014 Paris, France<sup>3</sup> Department of Physics and Astronomy, Iowa State University, Ames IA, 50011, USA<sup>4</sup> Service d'Astrophysique, CEA-Saclay, F-91191 Gif-sur-Yvette Cedex, France<sup>5</sup> Instituto de Astronomía y Física del Espacio, cc 67, suc 28, (1428) Buenos Aires, Argentina

Received 28 July 1998 / Accepted 21 October 1998

**Abstract.** We present the first detection of molecular gas in the Cartwheel, the prototype of a collisional ring galaxy formed in the head-on encounter of two galaxies. Until now, only very little atomic gas and no CO had been detected in the centre, where gas is theoretically expected to pile up. Using the Swedish ESO Submm Telescope, we detected both  $^{12}\text{CO}(1-0)$  and  $(2-1)$  line emission towards the central position. The line ratio and the line widths suggest that the  $\text{CO}(2-1)$  emission is sub-thermal and that the  $\text{CO}(1-0)$  emission arises within the central  $22''$  (13 kpc); it is probably associated with the inner ring and nucleus. We infer a mass of molecular gas ( $\text{H}_2$ ) of  $1.5$  to  $6 \cdot 10^9 M_\odot$ , which is significantly higher than the  $\sim 10^8 M_\odot$  of atomic gas within that region. The low excitation of the gas, whether it is due to a low temperature or a low density, is consistent with the weak star-forming activity observed in the centre of the Cartwheel.

**Key words:** galaxies: individual: AM0035-33 – galaxies: individual: The Cartwheel – galaxies: ISM – radio lines: galaxies

**1. Introduction**

The Cartwheel Galaxy, discovered by Zwicky (1941), earned its nickname from the prominent system of spokes which connects the bright outer ring to the inner ring (see Fig. 1). The nature of the Cartwheel was elucidated by early numerical simulations, which showed convincingly that such ring systems can form when a companion galaxy plunges through the centre of a larger rotating disk (Lynds & Toomre 1976; Theys & Spiegel 1976). The passage of the “intruder” triggers a ring-wave that propagates through the disk of the “target” galaxy and induces massive star formation in a well-defined ring.

In contrast to most merging galaxies in which star formation is significantly enhanced in a very small area (the very centre), ring galaxies exhibit starbursts on a large scale. Most observed ring galaxies have blue colours and elevated CO,  $\text{H}\alpha$ ,

far-infrared and radio continuum emission (see Appleton & Struck-Marcell 1996 for a review). Because of the simple geometry of the interaction, they appear as textbook examples to study the effects that a collision has on the interstellar medium of a galaxy and to follow the chronology of the star-formation in the expanding ring.

The Cartwheel Galaxy, because of its well-defined inner and outer rings, is considered as the prototype of its class. It has been the subject of several observational studies as well as dynamical modeling (Struck-Marcell & Higdon 1993; Hernquist & Weil 1993; Mihos & Hernquist 1994). Optical and near-IR imaging showed strong radial colour gradients in the disk interior to the outer ring, which may trace the evolution of the stellar population in the wake of the density wave (Marcum et al. 1992). HST images have revealed with unprecedented detail the distribution of massive young clusters in the outer ring, as well as the diffuse and knotty structure of the spokes (Borne et al. 1997; Appleton et al. 1998).

The outer ring of the Cartwheel ( $\sim 70''$  in diameter) is expanding, has blue colours and is populated by massive star-forming regions (Higdon 1995, Amram et al. 1998). Most of the star formation occurs in the southern quadrant of the ring, where the  $\text{H}\alpha$  emission, as well as the 20 cm and 6 cm radio continuum emission peak (Higdon 1996). Spectroscopy of a few H II regions in the outer ring indicates a low metallicity (Fosbury & Hawarden 1976). Most of the atomic gas (HI) is associated with the outer ring. The detection of a massive HI plume extending more than 80 kpc in projection in the direction of a companion galaxy (G3) suggests that G3 rather than one of the two nearer companions collided with the Cartwheel and produced its present-day appearance (Higdon 1996).

The inner ring ( $\sim 18''$  in diameter) and nucleus of the Cartwheel seem gas-poor and until recently, no evidence of star formation could be found. This is in disagreement with the models that predict an infall of gas towards the centre and vigorous star formation in the inner ring (Struck-Marcell & Appleton 1987). However, a number of recent observations has revealed a richer environment in the inner regions of the Cartwheel:

Send offprint requests to: C. Horellou

\* based on observations made with the Swedish-ESO Submillimeter Telescope (SEST) at La Silla, Chile

i) The HST images resolve a network of dust lanes in the inner ring and luminous kiloparsec-size cometary structures which are suggestive of massive dense clouds traveling through the ambient gas (Struck et al. 1996).

ii) H $\alpha$  emission has been detected at a low level throughout the inner ring and nucleus (Amram et al. 1998, Higdon et al. 1997).

iii) ISOCAM images show strong 7  $\mu$ m and 15  $\mu$ m emission in the inner ring and nucleus. The mid-IR fluxes indicate the presence of hot dust and are consistent with weak star formation activity (Charmandaris et al. 1998).

These new results strengthened our expectation that molecular gas must be present in the central region of the Cartwheel. Previous searches for  $^{12}\text{CO}(J=1-0)$  line emission had been unsuccessful, and the Cartwheel was one of the two galaxies that remained undetected in the survey of 16 ring galaxies of Horellou et al. (1995). Here, we present the first  $^{12}\text{CO}(1-0)$  and  $^{12}\text{CO}(2-1)$  detections towards the centre of the Cartwheel. For  $H_0=75 \text{ km s}^{-1} \text{ Mpc}^{-1}$ , the distance to the galaxy is 121 Mpc.

## 2. Observations and data reduction

We have observed at  $\alpha=00\text{h}37\text{m}40.8\text{s}$ ,  $\delta=-33^\circ42'56.9''$  (J2000), which is the peak of emission of the Cartwheel nucleus in the HST I-band image.

The observations have been carried out in July 1998 in La Silla (Chile) with the 15m Swedish-ESO Submillimeter Telescope (SEST) (Booth et al. 1989). We used the IRAM 115 and 230 GHz receivers to observe simultaneously at the frequencies of the  $^{12}\text{CO}(1-0)$  and the  $^{12}\text{CO}(2-1)$  lines. At 115 GHz and 230 GHz, the telescope half-power beam widths are 43'' and 22'', respectively. The main-beam efficiency of SEST is  $\eta_{\text{mb}} = T_{\text{A}}^*/T_{\text{mb}}=0.68$  at 115 GHz and 0.46 at 230 GHz (SEST handbook, ESO). The typical system temperature varied between 220 and 320 K (in  $T_{\text{A}}^*$  unit) at both frequencies. The total on-source integration time was 6 hours. A balanced on-off dual beam switching mode was used, with a frequency of 6 Hz and two symmetric reference positions offset by 12' in azimuth. The pointing was regularly checked on the SiO maser R Aqr. The pointing accuracy was 4'' rms. The backends were low-resolution acousto-optical spectrometers. The total bandwidth available was 500 MHz at 115 GHz and 1 GHz at 230 GHz, with a velocity resolution of 1.8  $\text{km s}^{-1}$ . The data were reduced with the software CLASS. Only first-order baselines were subtracted from the spectra.

## 3. Results and discussion

In Fig. 1 we present the CO(1-0) and CO(2-1) spectra obtained towards the centre of the Cartwheel, as well as the HST image (Borne et al. 1996) on which the sizes of the CO beams have been superimposed. The parameters of the lines, derived from gaussian fits after smoothing to a final velocity resolution of 15  $\text{km s}^{-1}$ , are given in Table 1. The central velocities agree with the systemic velocity of 9089  $\text{km s}^{-1}$  determined from H I observations (Higdon 1996). An indicative molecular gas mass

**Table 1.** Observational results.

| Line    | $v_{\text{hel,opt}}$<br>$\text{km s}^{-1}$ | $\Delta v$<br>$\text{km s}^{-1}$ | $\int T_{\text{mb}} dv$<br>$\text{K km s}^{-1}$ | $\sigma_{\text{mb}}$<br>$\text{mK}$ | $M(\text{H}_2)$<br>$10^9 M_{\odot}$ |
|---------|--|----------------------------------|---|-------------------------------------|-------------------------------------|
| CO(1-0) | 9123 $\pm$ 13                              | 218 $\pm$ 23                     | 0.82 $\pm$ 0.10                                 | 1.0                                 | 1.5                                 |
| CO(2-1) | 9136 $\pm$ 12                              | 211 $\pm$ 27                     | 0.95 $\pm$ 0.11                                 | 1.2                                 |                                     |

within the CO(1-0) beam is given in the last column of Table 1. It has been computed using a standard CO-H $_2$  conversion factor (see below).

### 3.1. Molecular gas mass and CO(2-1)/(1-0) line ratio

To convert CO intensities into H $_2$  column densities, we use the factor of Strong et al. (1988):

$$X = N(\text{H}_2)/I_{\text{mb}}(\text{CO}) = 2.3 \cdot 10^{20} \text{ mol cm}^{-2} (\text{K km s}^{-1})^{-1} \quad (1)$$

where  $I_{\text{mb}}(\text{CO}) = \int T_{\text{mb}} dv$  is the main-beam line area. This yields a mass

$$M(\text{H}_2) (M_{\odot}) = 1.25 \cdot 10^5 (\theta/43'')^2 I_{\text{mb}}(\text{CO}) (D/1\text{Mpc})^2 \quad (2)$$

where  $\theta$  is the half-power beam width of the telescope.

From the CO(1-0) line intensity, we estimate a mass of molecular gas (H $_2$ ) of 1.5  $10^9 M_{\odot}$  within the 43'' beam. This value should be interpreted with caution since it is known that the CO-to-H $_2$  conversion factor ( $X$ ) is dependent on the metallicity (e.g. Maloney & Black 1988). Due to the very weak line emission in the centre, the metallicity could be measured only in the outer star-forming ring of the Cartwheel, and it is  $12+\log[\text{O}/\text{H}]=8.1$  (Fosbury & Hawarden 1976), compared with 8.9 in Orion. If the nucleus has the same metallicity as the outer ring, then the conversion factor would be higher than the standard one by a factor of about 4 (Wilson 1995), and the H $_2$  mass as well. However, it is also known that most galactic disks present a metallicity gradient, with metallicities in the nucleus up to  $\sim 10$  times higher than in the outer parts of the disk (Smartt & Rolleston 1997). Although  $X$  may vary linearly with the reciprocal of metallicity when the metallicity is low,  $X$  is expected to become less sensitive to metallicity at values above that of Orion (Sakamoto 1996). Thus, if we take into account the metallicity gradient across the disk, the value of  $X$  for the nucleus of the Cartwheel might be not much lower than the standard value. We can bracket the conversion factor in the nucleus:  $X < X_{\text{nucl}} < 4X$ , and the H $_2$  mass within the 43'' beam:  $1.5 \cdot 10^9 < M(\text{H}_2) [M_{\odot}] < 6 \cdot 10^9$ .

H $_2$  masses in this range are common for central regions of normal spirals of intermediate and late types (e.g., see Fig. 133 in Young et al. 1995) and are similar to those inferred for other ring galaxies (Horellou et al. 1995).

More unusual is the fact that we observe similar integrated intensity in the CO(1-0) and CO(2-1) lines, despite the difference of a factor of 4 in the beam areas. If the CO lines were thermalized, this would imply that the surface density of the CO

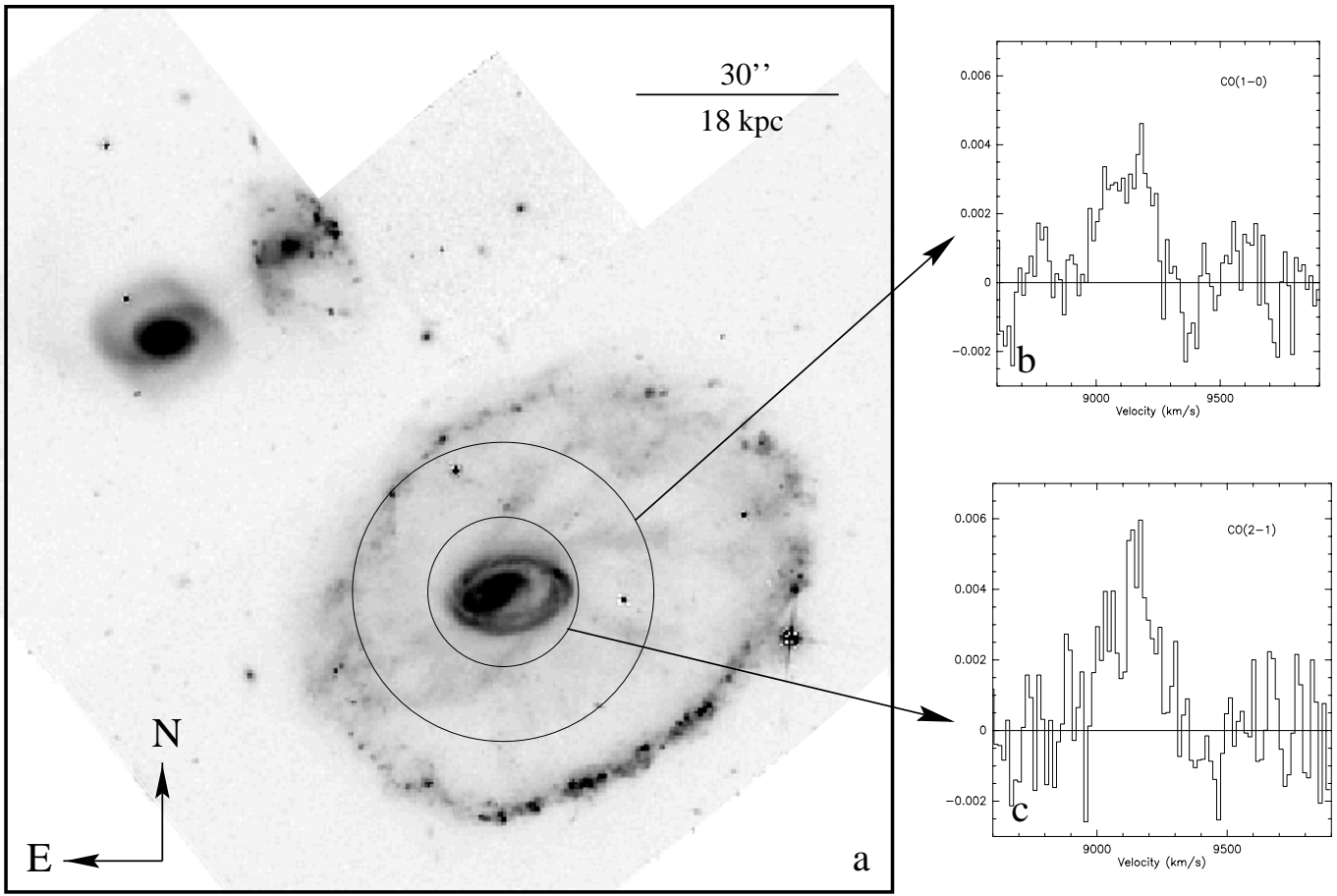


**Fig. 1.** **a** HST I-band image of the Cartwheel galaxy (Borne et al. 1996). The circles on the optical image represent the resolution of the CO(1–0) and CO(2–1) observations (43'' and 22'' respectively). **b** The CO(1–0) spectrum of the nuclear regions. The  $y$ -axis shows the main-beam temperature in K. The velocity resolution is  $15 \text{ km s}^{-1}$ . **c** The CO(2–1) spectrum. Units and velocity resolution are the same as in **b**.

gas would be nearly constant within the 25 kpc CO(1–0) beam diameter, which is very improbable. The surface density of most disk galaxies shows an exponential radial decrease. Even if the spokes were gas-rich, as some numerical simulations predict (Hernquist & Weil 1993, Mihos & Hernquist 1994), their filling factor is likely to be low. For a linear decrease of the surface density, one expects a line ratio of 0.5. We rather suggest that the CO(2–1) emission is sub-thermal, possibly because of a low temperature or a low gas density, and that the CO emission is concentrated within the 13 kpc CO(2–1) beam (which is consistent with the fact that both lines have similar widths). Correcting for the different beam sizes, one obtains a CO(2–1)/CO(1–0) line ratio of  $0.3 \pm 0.05$ , which is significantly lower than the ratio of 0.9 observed in nearby spirals (Braine & Combes 1992). Such low ratios have been observed in dark clouds of M31 where there is little evidence of star-forming activity (Allen & Lequeux 1993).

### 3.2. Comparison of CO, H I and H $\alpha$ emission

Let us try to compare the spatial distribution and kinematical signature of the CO gas with those of the atomic and the

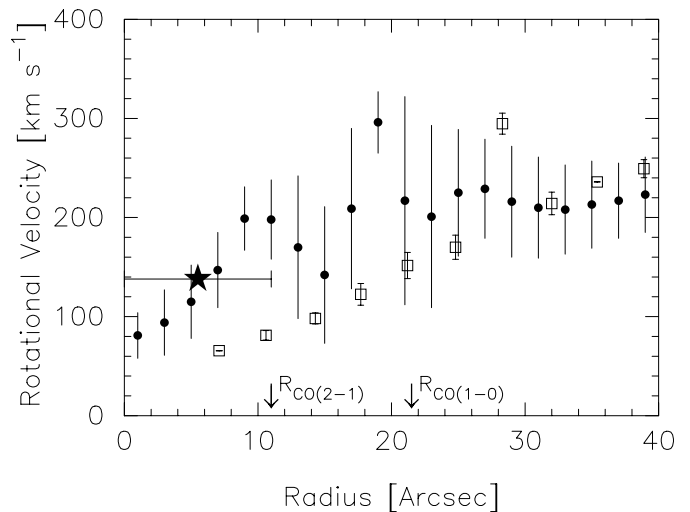


**Fig. 2.** The rotation curve of the Cartwheel assuming an inclination of  $50^\circ$ . The open squares are the H I values (Higdon 1996), the filled circles are the H $\alpha$  points (Amram et al. 1998) and the filled star is the velocity derived from the CO(2–1) line width. The arrows on the  $x$ -axis indicate the radii of the beams of the CO(1–0) and CO(2–1) observations.

ionized hydrogen. Neutral hydrogen is undetected within the central  $R = 10''$  of the galaxy ( $\Sigma(\text{HI}) < 0.3 \text{ M}_{\odot} \text{ pc}^{-2}$ ) and has a roughly constant surface density from  $R = 10''$  to  $22''$ . ( $\Sigma(\text{HI}) \approx 4 \text{ M}_{\odot} \text{ pc}^{-2}$ , Higdon 1996). The HI mass within our  $43''$  CO(1–0) beam is  $1.5 \cdot 10^9 \text{ M}_{\odot}$ , which is of the same order as the molecular gas mass that we have calculated, but it is only  $\sim 10^8 \text{ M}_{\odot}$  within the  $22''$  CO(2–1) beam. If, as argued in the previous paragraph, the CO emission is concentrated, then the interstellar medium within the central  $22''$  is predominantly molecular.

The HI rotation curve rises smoothly from the inner to the outer ring (see Fig. 2). Atomic gas is infalling near the inner ring, where HI concentrations are seen. Assuming that the CO gas is distributed in an inclined plane ( $i \sim 50^\circ$ ), we can use the line widths to estimate the rotational velocity in the central region of the galaxy. For the CO(2–1) line we find  $v_{R21} = \Delta v / 2 \sin i = 138 \text{ km s}^{-1}$  which is significantly higher than the velocities measured for the HI gas at radii  $R < 20''$  (see Fig. 2). The CO point is more consistent with the  $\text{H}\alpha$  rotation curve. The difference between the HI velocity on one hand and the  $\text{H}\alpha$  and CO velocities on the other hand is likely to be due to different distributions of the atomic and molecular gas, the latter being more concentrated.

#### 4. Conclusion

We have presented the first detection of  $^{12}\text{CO}(1-0)$  and  $^{12}\text{CO}(2-1)$  line emission towards the nucleus of the Cartwheel galaxy and estimated the mass of molecular gas within the central  $43''$  ( $1.5 \cdot 10^9 < M(\text{H}_2) < 6 \cdot 10^9 \text{ M}_{\odot}$ ). The limited angular resolution of these single-dish observations does not allow us to determine precisely the location of the molecular gas, but it is probably concentrated within the central  $22''$  where little atomic gas is found ( $\sim 10^8 \text{ M}_{\odot}$ , Higdon 1996). The CO(2–1) to (1–0) line ratio is low, suggesting sub-thermal excitation, which is consistent with the low level of star-forming activity observed in the central region of the Cartwheel. These CO measurements make it possible to justify future interferometric observations to study the distribution and the dynamics of the molecular gas with a better spatial resolution and to establish whether it is associated with the inner ring and/or the dust-lanes, and whether it is of pre-collisional origin or infalling onto the nucleus as numerical simulations predict.

*Acknowledgements.* We are grateful to L.-Å. Nyman and to the SEST staff for the support during the observations, to S. Leon (Observa-

toire de Paris), C. Struck (Iowa State University) and J.H. Black (Onsala Space Observatory) for useful discussions and comments. C.H. acknowledges financial support from the Swedish Natural Science Research Council (NFR). V.C. acknowledges the financial support from the TMR fellowship grant ERBFMBICT960967. We would like to thank an anonymous referee for critical comments on the manuscript.

#### References

- Allen, R.J. & Lequeux, J., 1993, ApJ 410, L15  
 Amram, P., Mendes de Oliveira, C., Boulesteix, J. & Balkowski, C., 1998, A&A 330, 881  
 Appleton, P.N. & Struck-Marcell, C., 1996, Fund. of Cos. Phys. 16, 111  
 Appleton, P.N., et al., 1998, in *Galaxy Interactions at Low and High Redshift*, IAU 186, in press.  
 Booth, R., Delgado, G., Hagström, M., et al. 1989, A&A 216, 315  
 Borne, K.D., Lucas, R., Appleton, P.N. et al., 1996, in *Science with the Hubble Space Telescope II*, edited by P. Benvenuti, F.D. Macchetto, and E.J. Schreier, (STScI, Baltimore)  
 Borne, K. et al., 1997, Rev. Mex. Astron. Astrofis. 6, 141  
 Braine, J., Combes, F., 1992, A&A 264, 433  
 Charmandaris, V. et al., 1998, A&A, in press  
 Fosbury, R. & Hawarden, T., 1976, MNRAS 178, 473  
 Higdon, J.L., 1995, ApJ 455, 524  
 Higdon, J.L., 1996, ApJ 467, 241  
 Higdon, J.L., Cecil, G., Bland-Hawthorn, J., Lord, S.D., 1997, AAS 191, 8907  
 Hernquist, L. & Weil, M., 1993, MNRAS 261, 804  
 Horellou, C., Casoli, F., Combes, F. et al., 1995, A&A 298, 743  
 Lynds, R. & Toomre, A., 1976, ApJ 209, 382  
 Maloney, P., & Black, J.H., 1988, ApJ 325, 389  
 Marcum, P., Appleton, P. N., & Higdon, J., 1992, ApJ 399, 57  
 Mihos, J.C., & Hernquist, L., 1994 ApJ 437, 611  
 Sakamoto, S., 1996, ApJ 462, 215  
 Smartt, S.J., Rolleston, W.R.J., 1997, ApJ 481, L47  
 Strong, A.W., Bloemen, J.B.G.M., Dame, T.M., et al., 1988, A&A 207, 1  
 Struck, C., Appleton, P.N., Borne, K.D., & Lucas, R.A. 1996, AJ 112, 1868  
 Struck-Marcell, C. & Appleton, P.N., 1987, ApJ 323, 480  
 Struck-Marcell, C. & Higdon, J.L., 1993, ApJ 411, 108  
 Theys, J. & Spiegel, E., 1976, ApJ 212, 616  
 Thronson, H.A.Jr. & Telesco, C.M., 1986, ApJ 311 98  
 Wilson, C.D., 1995, ApJ 448, L97  
 Young, J., Shuding Xie, Tacconi, L. et al., 1995 ApJS, 98, 219  
 Zwicky, F., 1941, in Th. von Karman Anniversary volume, p. 137, Contribution to Applied Mechanics and Related Subjects, California Institute of Technology, Pasadena